



OpenAIR@RGU

The Open Access Institutional Repository at Robert Gordon University

<http://openair.rgu.ac.uk>

This is an author produced version of a paper published in

Materials & Design (ISSN 0261-3069)

This version may not include final proof corrections and does not include published layout or pagination.

Citation Details

Citation for the version of the work held in 'OpenAIR@RGU':

GENDRE, L., NJUGUNA, J., ABHYANKAR, R. and ERMINI, V., 2015. Mechanical and impact performance of three-phase polyamide 6 nanocomposites. Available from *OpenAIR@RGU*. [online]. Available from: <http://openair.rgu.ac.uk>

Citation for the publisher's version:

GENDRE, L., NJUGUNA, J., ABHYANKAR, R. and ERMINI, V., 2015. Mechanical and impact performance of three-phase polyamide 6 nanocomposites. *Materials & Design*, 66 (B), pp. 486-491.



This work is licensed under a Creative Commons Attribution - Non-Commercial - No-Derivatives 4.0 International Licence

Copyright

Items in 'OpenAIR@RGU', Robert Gordon University Open Access Institutional Repository, are protected by copyright and intellectual property law. If you believe that any material held in 'OpenAIR@RGU' infringes copyright, please contact openair-help@rgu.ac.uk with details. The item will be removed from the repository while the claim is investigated.

Mechanical and impact performance of three-phase polyamide 6 nanocomposites

Laura Gendre¹, James Njuguna^{2*}, Rishi Abhyankar¹ and Valentina Ermini³

¹Centre for Automotive Technology, Cranfield University, Bedford, MK43 0AL, UK

²Institute for Innovation, Design and Sustainability, School of Engineering, Robert Gordon University, Aberdeen, AB10 7GJ, UK

³Laviosa Chimica Mineraria, Via Leonardo da Vinci, 21 I-57123 Livorno, Italy

* Corresponding author (E: j.njuguna@rgu.ac.uk, T: +44 (0) 122 426 2304)

Abstract

In this work, three-phase nanocomposites using multiscale reinforcements were studied to evaluate the influence of nanofillers on static and dynamic mechanical properties at varying temperature conditions. In particular, short-fibres reinforced polyamide 6 (30 wt.%) composites with various weight fractions of montmorillonite (OMMT) and nanosilica (SiO₂), manufactured and investigated. Quasi-static tensile properties were investigated at room temperature and also at 65°C just above the polyamide 6 (PA6) glass transition temperature. The low velocity impact tests were conducted on the manufactured cone-shaped structures to evaluate the crash behaviour and energy absorption capability. The study results shows that the increase of the weight percentage level of OMMT in PA6/glass fibre (30 wt.%) composite made the nanocomposites more brittle and simultaneously deteriorated the tensile properties. SiO₂ nanofiller at 1 wt.% was found to be the optimum ratio for improving tensile properties in silica-based nanocomposites studied. It was further noted that for both types of nanofillers, the crashing behaviour and energy absorption in dynamic properties were improved with increase in nanofillers weight percentage in the composites. The study also shows that the brittleness behaviour of the nanocomposites investigated is associated to the fibre/matrix interaction which is dependent on the nanofiller type and has significant effect on crash modes observed.

Keywords: Three-Phase Nanocomposites, Polyamide 6, Impact Performance, Mechanical properties.

1 Introduction

A significant number polymer and polymer composites are increasingly being used in various industrial applications such as, aerospace, automotive and chemical industries. This is because these materials provide high strength/weight ratio in comparison to classic material. In addition, most classic polymer materials have limited structural applications due to their low mechanical, thermal and impact resistance properties. Therefore reinforcements are often used to improve their properties [1, 2].

Today, various types of polyamides covering a wide range of properties are commercially available. Polyamide 6 (PA6) is one of the polyamides grades most widely used in the automotive industry. PA6 is a high performance engineering thermoplastic used in electrical/electronics, automobile, packaging, textiles and consumer applications. However, limitations in mechanical properties, the low heat deflection temperature, high water absorption and dimensional instability of pure PA6 have prevented its wide range applications in load bearing applications such as under-the-hood automotive applications [3]. Hence, polyamide 6 reinforcement using nanofillers to further widen and increase its application range in impact/crash applications is beneficial [4].

In brief, nanocomposite materials are an attractive technology because using nano-fillers allows great improvements of the polymeric materials compared to micro-reinforcement and suit to the industrial/technological goals [5]: e.g. to produce lighter, thinner, stronger and cheaper structures [6]. The nano-size of the fillers increases the area of contact between matrix and filler and so, reduces stress concentration around the filler. Also, the nano-size presents a very large surface area to volume ratio. For example, it augments the surface area to volume ratio up to 10^3 times for a nanofibre compared to a microfiber [6]. It is also significant to note that only 5 wt. % of nanofillers can significantly improve behaviour and properties of a neat polymer [7], compared to at least 20 wt. % with glass fibre reinforcement,

which allows a reduction of weight and cost. For the nano-reinforced composites, however, it is essential to control and stabilize a desired type of morphology in polymers in order to generate polymeric materials with favorable properties.

Some of the key properties that are improved include strength, stiffness, heat-distortion temperature, scratch resistance, thermal, oxidative and dimensional stability, water and thermal permeability, corrosion resistance, surface hardness, barrier properties, flame retardancy and electrical conductivity [8, 9]. Some studies in the literature have focused their research on the influence of modified or unmodified clay on polymer nanocomposites' properties [10–14]. For example, enhancement of mechanical properties of nanocomposites and three-phase nanocomposites are often confirmed. Mishra *et al.* [13] had shown that Young modulus, tensile strength and elongation at break are increasing with the augmentation of organically modified montmorillonite (OMMT) content (until 3 wt. %) into a polyamide-66 matrix. Silva *et al.* [15], reported that an increase of 32% for the elongation at break for a 30 wt. % glass fibre/polyamide-6 filled with 2 wt. % of SiO₂ nanoparticles, compared to a classical polyamide-6/glass fibre. Wu *et al.* [16] found that a polyamide-6/clay with 30 wt.% of glass fibre had an enhanced tensile strength of 11% and a tensile modulus enhancement of 42% compared to polyamide-6/ 30wt.% glass fibre. Further, several parameters were demonstrated to have an influence on these mechanical properties (stiffness, modulus) such as interaction between the matrix and the fillers [17], fillers' size [18], fillers' volume fraction [19], and filler's shape [9]. Others advantages are the cost which is low considering that only a small amount of filler is necessary, and the ease of manufacture without need to change the conventional processing conditions in order to manufacture new products [6].

As the use of thermoplastics in the automotive industry increases, the need to determine their impact responses to ensure safety and stability of designed structures is important. As such,

the impact test should be ideally designed to simulate the loading conditions to which the composite component is subjected in operational service and then reproduce the failure modes and mechanisms likely to occur in real conditions. More efforts in understanding the impact performance and failure mechanisms of reinforced thermoplastics used in automotive industry are necessary. As nano and micro sized fillers can reinforce polymer property in different aspects, combining both into one three-phase composite is increasingly considered as a promising solution for future lightweight structures. Despite the fact that the mechanical properties of two phase composites have been extensively studied in the available literature, it is very difficult to predict how a three phase material will behave under the same conditions. This present study therefore aims to investigate the morphology and the mechanical properties of PA6-based three phase composites filled with different nano or micro materials and short glass-fibres. The effects of the polymer matrices and reinforcement materials on the mechanical properties of injection moulded composites were studied and discussed. In particular, the influence of the nano-fillers content and temperature changes in three-phase nanocomposites using multiscale reinforcements were studied. Polyamide-6 reinforced filled with short glass fibre 30 wt.% and with an addition of nanoclay (montmorillonite, OMMT) and/or nanosilica (SiO_2) were tested in order to characterise their tensile properties at room temperature and at 65°C just above the polyamide 6 glass transition temperature. The quasi-static tensile properties are complemented with crashing behaviour ones and fracture studies were also conducted for completeness.

2 Experiment

2.1 Materials and samples preparation

Glass-fibre reinforced polyamide MM-PA I 1F30 i.e. polyamide-6 (Durethan B30 and B31) reinforced by 30% of glass fibre (ThermoFlow672) were supplied by MACOMASS Verkaufs AG Germany. Montmorillonite, Dellite 43B, were obtained from Laviosa Chemicals. Fumed silica nanoparticles AEROSIL 974 were obtained from Degussa.

Two types of three-phase nanocomposites were produced: polyamide-6 (Durethan B30) reinforced by 30% of glass fibre (ThermoFlow672) and particles of SiO₂ (Aerosil R 974), and polyamide-6 reinforced by 30 wt.% of glass fibre (GF) and montmorillonite (Dellite 43B, Laviosa Chemicals). Preparation of nano and glass reinforced polymer composites was conducted in three main steps: preparation of nano-composite granulate, mixing and extrusion of nano and glass reinforced composite granulates and injection moulding of macro-samples. A flow chart showing the preparation process. In total, seven materials were manufactured with different content of nano-fillers (Table 1).

Table 1

The mechanical testing specimens were obtained by direct melting and extrusion in a twin-screw extruder at a maximum temperature of 280°C. The product was cooled in a water bath, pelletized and then dried. From granulates, test samples (crash cones, tensile bars and plates) were manufactured by injection moulding according to the ISO 527 [20] test standard requirements.

2.2 Mechanical testing

Quasi-static and dynamic tensile tests were carried out using Instron 5500R universal testing machine. All experiments were conducted according to ISO-527 [20] standard, using specimen type A. Samples were machined from injection moulded plates in two different direction: longitudinal (along fibres) and transverse (cross-fibre). Five samples of each material were tested at crosshead speed of 0.1 mm/min. The load was measured using a 100kN load cell. In order to measure the strain a laser extensometer was used.

Crashing behaviour was analysed with quasi-static and dynamic crash experiments. Quasi-static compression testing of the crash cones was carried out using Instron 5500R universal testing machine. A set of samples of each material were tested at a crosshead speed of 0.1mm/sec. The load was measured using 100kN load cell and the displacement was measured using a built in crosshead displacement sensor. Impact tests of the crash cones were carried out on a high energy capacity drop tower. Three samples of each material were tested at the velocity of 4.4 m/s. The tests were performed by direct impact of the falling beam. In order to ensure a good distribution of the load, 8mm thick steel plate was placed on the top surface of the cone. The impactor mass of 54 kg was constant in all tests, giving the overall impact energy of 522J. The load was measured using 200kN load cell, placed underneath the sample. In order to measure shortening of the sample (falling beam displacement), the linear variable differential transformer (LVDT) displacement transducer was used, with precision of 0.01mm and maximum displacement speed of 10m/s. The impact event was recorded using Phantom high speed camera.

2.3 Scanning Electron Microscopy

In order to study the materials failure mechanism and the relation between the matrix and the filler, the fracture surface of the tensile bars was examined with FEI XL30 field emission scanning electron microscope (FE-SEM). The operating voltage was in the range of 10-20 kV and the specimens were gold sputtered to minimize charging of the sample.

3 Results and discussion

3.1 Tensile properties

Effect of the filler's type

In this work, tensile properties of polyamide-6/glass fibre nanocomposites were investigated. Figure 1 illustrates the tensile stress vs tensile strain curves for the OMMT-based nanocomposites (Figure 1 (left)), and for the silica-nanocomposites (Figure 1 (right)) an ultimate strength and strain at break significantly higher than the OMMT-nanocomposites.

Figure 1

The materials showed a behaviour corresponding to a brittle material without yield point for both filler types tested. It was observed that the choice of the filler integrated to the polyamide-6/glass fibre composite is an important factor for tensile properties. The polyamide-6/glass fibre/OMMT deformed less, the stress vs. strain curves shows only elastic deformation followed by a brittle behaviour. Whereas the SiO₂-nanocomposites were less brittle and showed a plastic deformation before breaking it is also important to note that OMMT-based composites is stiffer than the silica-based ones.

Effect of the fillers' content

The main results of the tensile tests for OMMT-nanocomposites are listed in Table 2.

Table 2

It can be observed that the Young's Modulus was improved with increasing OMMT concentration at the expense of its ability to resist high loading and consequently lead to deformation failure at lower stress and strain values as the material became more brittle. These results can be explained by the effects of high content of nanofillers in the matrix. Akkapeddi [21], found that above 7 wt.% of nanoclay, polyamide-6 nanocomposites tend to present more fillers aggregates, and he suggested the use of a nano-content less than 5 wt.% in order to avoid these agglomerates. This may as well give a suitable explanation for the significant difference found for the tensile strain at break between a nanocomposite filled with 2 wt.% of nanoclay and the ones filled with a percentage superior to 5wt.%.

The SiO₂-nanocomposites were prepared at low content of nanofillers (between 0.5 and 3wt.%). Results of the tensile tests for SiO₂-nanocomposites are presented in Table 3.

Table 3

At room temperature, it is seen that the glass fibre-filled composites with 1 wt.% of nano-SiO₂ material have the best properties. Further, this is the only nanocomposite which showed an improvement in both the tensile strength, tensile, strain at break and the modulus compared to glass fibre/polyamide-6. These results are in line with the findings of Zhou *et al.*

[22], for nano-silica/polypropylene composites. They reported an optimum between 0.4 and 0.8 vol.% of SiO₂ depending on the treatment undergone by the filler.

Effect of the temperature

Figure 2 shows the difference between the tensile stress vs tensile strain curves at room temperature and also that at 65°C for the polyamide-6/glass fibre filled with 5 wt.% of OMMT content and the one filled with 1.5wt.% of SiO₂.

Figure 2

It can be noticed that the shape of the stress-strain curve is similar for the OMMT-nanocomposites and the SiO₂-nanocomposites, even if the values are still lower for the OMMT one.

For OMMT-nanocomposites, the same trend concerning the nanofillers percentage (Table 2) can be noticed at 65°C whereas it is different at room temperature. However, at 65°C the material is more ductile than at room temperature as expected which is a typical behaviour for a polymeric material especially when the temperature is above its glass transition. For polyamide-6 matrix, the glass transition temperature was reported to be between 40°C and 50°C [23]. The modulus is reduced by 50% at 65°C, the tensile strength is lower, and its strain at break increases by 2.5 folds. The SiO₂-based nanocomposites also behaved as a ductile material at 65°C to our expectations although the Young's modulus increased with the SiO₂ content. The tensile strength and strain at break followed the same trend to that at room temperature and consequently decreased with increase of nano-silica content.

The SEM investigations were conducted to study the fracture behaviour of the nanocomposites. For the OMMT-nanocomposites specimens studied at room temperature significant fibre pull-out was observed (Figure 3a).

Figure 3

The matrix underwent only elastic deformation, and one can notice that the surface is typical from a brittle fracture. However, Figure 3b shows that the matrix was plastically deformed for silica-nanocomposites at room temperature. The matrix/fibre adhesion was much stronger (Figure 3c) such that the glass fibres had to break instead of just pulling-out of the matrix. This explains the higher tensile strength of nano-silica reinforced polyamide observed tensile testing as observed elsewhere in the literature [16].

The fractured surfaces of the tensile bars tested at 65°C for both OMMT and nano-silica composites correspond to a ductile fracture with plastic deformation and drawing of the matrix. Significant fibre breakage was observed in general accompanied by only limited fibre pull-out. Nevertheless more clean fibres were observed for OMMT-nanocomposites at 65°C (than those nano-silica composites) signifying lower fibre/matrix interaction. For the nano-silica composites significant matrix' traces were found stuck on the fibre (Figure 3f), which again can explain [9] the higher tensile strength for these materials compared to the composites with OMMT nanofiller.

3.2 Crashing behaviour

The crashing behaviour was studied with quasi-static and dynamic crash tests. The results are presented in Table 4 and 5.

Table 4

Table 5

A reasonable method to classify the failure modes was identified by Silva et al. [24]: Mode I – progressive crushing with micro-fragmentation and delamination, Mode II – brittle fracture with large fragmentation and failure, Mode III – brittle but progressive crushing with medium fragmentation. The analysis of the results for the compressive experiments showed that all the nanocomposites had similar failure behaviour: brittle but progressive crushing with medium fragmentation (Figure 4b).

Figure 4

However, major cracks along the structure appeared in the cones made of polyamide-6/glass fibre/OMMT (Figure 4a), which led to a reduction of absorbed energy.

In the case of axial dynamic crash, the samples in polyamide-6/glass fibre/OMMT presented a better failure mode primarily through delamination as shown on Figure 4c, which involves an increase in energy absorption. It was noted that the energy absorption was improved when with increase of the OMMT content in the nanocomposites.

On the opposite, crash cones with a low percentage of SiO₂ had very poor fracture dispersion, which was highly brittle resulting into produced large fragmentation due to catastrophic failure (Figure 3c-d). However, it was noticed that that the energy absorption was enhanced when the nano-fillers percentage was increased and that polyamide-6/glass fibre and 3wt.% SiO₂ presented the best crash characteristics with an improved capacity of energy absorption and the desirable fracture mode with delamination.

Figure 5 and Figure 3c show the surface fracture of the polymer with the different nano-fillers.

Figure 5

In case of polyamide-6/glass fibre/OMMT, fibre pull-out was dominant and with no resins attached to their surfaces (clean), see Figure 5. The matrix underwent elastic deformation only hence the interaction between the glass fibre and the matrix was considerable poor. The opposite behaviour was noted for the materials with glass fibre and SiO₂ as the matrix was plastically deformed and interaction of fibres and matrix much attached to the fibre surfaces (Figure 3c) and is in agreement with recent studies [15]. Fibre/matrix bonding for nano-silica reinforced polyamide was stronger and the glass fibres had to break instead of just pulling-out of the matrix which in turn led to the reported higher impact and tensile strength.

4 Conclusions

The aim of this study was to identify the effect of the nano-fillers (type and content) on mechanical properties as well as the influence of the temperature. It was shown that the increase of OMMT percentage in polyamide-6/glass fibre composite made the material more brittle and had a negative effect on the tensile properties. This was explained by the weak interaction between the matrix and the fibres observed in the SEM images. The high content also led to nanofillers aggregates and hence a brittle material behaviour. For the addition in polyamide-6/glass fibre/nano-silica composites, the nanocomposites with 1 wt.% of SiO₂ presented the best tensile properties. As for classic polymeric materials, increasing the temperature (up to 65°C) made all the nanocomposites more ductile as expected and this was also confirmed by the SEM images.

Studies on the effect of the nano-fillers content on mechanical properties and failure behaviour showed that the increase of OMMT in polyamide-6/glass fibre composite influenced the brittleness of the material and had a negative effect on the tensile properties and quasi-static crashing behaviour. This is associated to the weak interaction between the matrix and the fibres. However, in dynamic crash tests, these samples presented significant delamination, and the energy absorption increased with OMMT content in the composites. Further, the nano-silica addition in polyamide-6/glass fibre, the nanocomposite with 1wt.% of SiO₂ presented the best tensile properties which were also the case for the quasi-static crashing behaviour. The polyamide-6/glass fibre/ 3wt.% SiO₂ enhanced mechanical properties showed preferred failure modes dominated by delamination during dynamic crashing. In general, it can be said that integration of secondary nanofillers is a positive means to enhance the mechanical properties of PA composites as long as the material

designer is conscious of the filler selection as well as the nanofiller weight percentage level which do play a crucial role in final desired properties.

Acknowledgement

This work was funded by the European Commission (NEPHH FP7 Project- CP-FP; Project Reference: 228536– 2) and from EC E-Life+11 ENV/ES/596 - Simulation of the release of nanomaterials from consumer products for environmental exposure assessment (SIRENA) and the European Community Action Scheme for the Mobility of University Students Erasmus Programme support to L Gendre.

References

- [1] J. Njuguna and K. Pielichowski, 'Polymer Nanocomposites', in *Structural Materials and Processes in Transportation*, -Ing Dirk Lehmus, -Ing thias Busse, -Ing Axel S. Herrmann, and K. Kayvantash, Eds. Wiley-VCH Verlag GmbH & Co. KGaA, 2013, pp. 339–369.
- [2] A. S. Herrmann, A. Stieglitz, C. Brauner, C. Peters, and P. Schiebel, 'Polymer Matrix Composites', in *Structural Materials and Processes in Transportation*, -Ing Dirk Lehmus, -Ing thias Busse, -Ing Axel S. Herrmann, and K. Kayvantash, Eds. Wiley-VCH Verlag GmbH & Co. KGaA, 2013, pp. 257–302.
- [3] Z. Mouti, K. Westwood, D. Long, and J. Njuguna, 'An experimental investigation into localised low-velocity impact loading on glass fibre-reinforced polyamide automotive product', *Compos. Struct.*, vol. 104, pp. 43–53, Oct. 2013.
- [4] J. Njuguna, *Structural Nanocomposites - Perspectives for Future Applications*. Springer Berlin Heidelberg, 2013, ISBN 978-3-642-40321-7.
- [5] PEN, 'CPI Home'. [Online]. Available: <http://www.nanotechproject.org/cpi/>. [Accessed: 17-Jun-2014].
- [6] J. Njuguna, K. Pielichowski, and S. Desai, 'Nanofiller-reinforced polymer nanocomposites', *Polym. Adv. Technol.*, vol. 19, no. 8, pp. 947–959, Aug. 2008.
- [7] C. Duval, 'Plastiques et automobile - D'aujourd'hui à demain'. *Techniques de l'ingenieur*, 10-Jul-2007.
- [8] D. Schmidt, D. Shah, and E. P. Giannelis, 'New advances in polymer/layered silicate nanocomposites', *Curr. Opin. Solid State Mater. Sci.*, vol. 6, no. 3, pp. 205–212, Jun. 2002.

- [9] J. M. Garcés, D. J. Moll, J. Bicerano, R. Fibiger, and D. G. McLeod, 'Polymeric Nanocomposites for Automotive Applications', *Adv. Mater.*, vol. 12, no. 23, pp. 1835–1839, 2000.
- [10] G. Jimenez, N. Ogata, H. Kawai, and T. Ogihara, 'Structure and thermal/mechanical properties of poly (ϵ -caprolactone)-clay blend', *J. Appl. Polym. Sci.*, vol. 64, no. 11, pp. 2211–2220, Jun. 1997.
- [11] T. Liu, K. Ping Lim, W. Chauhari Tjiu, K. P. Pramoda, and Z.-K. Chen, 'Preparation and characterization of nylon 11/organoclay nanocomposites', *Polymer*, vol. 44, no. 12, pp. 3529–3535, Jun. 2003.
- [12] Z.-Z. Yu, C. Yan, M. Yang, and Y.-W. Mai, 'Mechanical and dynamic mechanical properties of nylon 66/montmorillonite nanocomposites fabricated by melt compounding', *Polym. Int.*, vol. 53, no. 8, pp. 1093–1098, Aug. 2004.
- [13] S. Mishra, S. S. Sonawane, and N. G. Shimpi, 'Influence of organo-montmorillonite on mechanical and rheological properties of polyamide nanocomposites', *Appl. Clay Sci.*, vol. 46, no. 2, pp. 222–225, Oct. 2009.
- [14] F. Zhao, X. Bao, A. R. McLauchlin, J. Gu, C. Wan, and B. Kandasubramanian, 'Effect of POSS on morphology and mechanical properties of polyamide 12/montmorillonite nanocomposites', *Appl. Clay Sci.*, vol. 47, no. 3–4, pp. 249–256, Feb. 2010.
- [15] F. Silva, S. Sachse, and J. Njuguna, 'Mechanical properties and impact-energy absorption of injection moulded nanocomposites structures', presented at the ECCM15-15th European Conference on Composite Materials, Venice, Italy, 2012.
- [16] S.-H. Wu, F.-Y. Wang, C.-C. M. Ma, W.-C. Chang, C.-T. Kuo, H.-C. Kuan, and W.-J. Chen, 'Mechanical, thermal and morphological properties of glass fiber and carbon fiber

- reinforced polyamide-6 and polyamide-6/clay nanocomposites', *Mater. Lett.*, vol. 49, no. 6, pp. 327–333, Jul. 2001.
- [17] J. Njuguna, F. Silva, and S. Sachse, 'Nanocomposites for Vehicle Structural Applications', in *Nanofibers - Production, Properties and Functional Applications*, Tong Lin Ed., 2011.
- [18] C.B. Ng, L.S. Schadler, and R.W. Siegel, 'Synthesis and mechanical properties of TiO₂-epoxy nanocomposites', *Nanostructured Mater.*, vol. 12, no. 1–4, pp. 507–510, 1999.
- [19] F. Yang, Y. Ou, and Z. Yu, 'Polyamide 6/silica nanocomposites prepared by in situ polymerization', *J. Appl. Polym. Sci.*, vol. 69, no. 2, pp. 355–361, 1998.
- [20] 'ISO 527-1:2012 - Plastiques -- Détermination des propriétés en traction -- Partie 1: Principes généraux'. [Online]. Available: http://www.iso.org/iso/fr/home/store/catalogue_tc/catalogue_detail.htm?csnumber=56045. [Accessed: 17-Jun-2014].
- [21] M. K. Akkapeddi, 'Glass fiber reinforced polyamide-6 nanocomposites', *Polym. Compos.*, vol. 21, no. 4, pp. 576–585, 2000.
- [22] T. H. Zhou, W. H. Ruan, Y. L. Mai, M. Z. Rong, and M. Q. Zhang, 'Performance improvement of nano-silica/polypropylene composites through in-situ cross-linking approach', *Compos. Sci. Technol.*, vol. 68, no. 14, pp. 2858–2863, Nov. 2008.
- [23] R. F. Landel and L. E. Nielsen, *Mechanical Properties of Polymers and Composites, Second Edition*. CRC Press, 1993.
- [24] F. Silva, J. Njuguna, S. Sachse, K. Pielichowski, A. Leszczynska, and M. Giacomelli, 'The influence of multiscale fillers reinforcement into impact resistance and energy absorption properties of polyamide 6 and polypropylene nanocomposite structures', *Mater. Des.*, vol. 50, pp. 244–252, Sep. 2013.

Caption of Tables and Figures

Tables

Table 1: Composition of the different studied nanocomposites.

Table 2: Tensile properties of the OMMT-nanocomposites at room temperature and 65°C.

Table 3: Tensile properties of the SiO₂-nanocomposites at room temperature and 65°C.

Table 4 Quasi-static characteristics of the nanocomposites structures

Table 5 Dynamic crashing characteristics of the nanocomposites structures

Figures

Figure 1: Tensile stress vs tensile strain curves for polyamide-6/glass fibre/OMMT (right) and Polyamide-6/Glass Fibre/SiO₂ at different contents (left).

Figure 2: Tensile stress vs tensile strain curves for OMMT-nanocomposites (5 wt.%) and SiO₂-nanocomposites (1.5 wt.%) at room temperature and 65°C.

Figure 3: SEM pictures of the tensile fracture surface (a) OMMT-nanocomposite at room temperature, (b) silica-nanocomposite at room temperature, (d) OMMT-nanocomposites at 65°C, (e) silica-nanocomposite at 65°C, and zoom at the glass fibre for silica-nanocomposites (c) at room temperature, and (f) at 65°C.

Figure 4 Crash cones reinforced by OMMT, after compression test (a), after crash test (c), reinforced by nano-silica, after compression test (b), after crash test (d)

Figure 5: Typical fracture surface of PA6/GF/OMMT samples

Table 1: Composition of the different studied nanocomposites.

	Type of Matrix	wt.% of PA6	Type of Glass Fibre	wt.% of GF	Type of filler	wt.% of filler
HZ12-01	Durethan B30	65	ThermoFlow 672	30	Dellite 43B	5
HZ12-02	Durethan B30	62.5	ThermoFlow 672	30	Dellite 43B	7.5
HZ12-03	Durethan B30	60	ThermoFlow 672	30	Dellite 43B	10
HZ12-04	Durethan B30	69	ThermoFlow 672	30	Aerosil R 974	1
HZ12-05	Durethan B30	69.5	ThermoFlow 672	30	Aerosil R974	0.5
HZ12-06	Durethan B30	68.5	ThermoFlow 672	30	Aerosil R 974	1.5
HZ12-07	Durethan B31	67	ThermoFlow 673	30	Aerosil R 974	3

Table 2: Tensile properties of the OMMT-nanocomposites at room temperature and 65°C.

	Percentage of Nanofillers	Young's Modulus (GPa)		Tensile Strength (MPa)		Tensile Strain at break (%)		Reference
		RT	65°C	RT	65°C	RT	65°C	
PA + GF + OMMT	0%	6.92	-	116.2	-	5.2	-	[15]
	2%	7.61	-	109.7	-	5.1	-	[15]
	5%	9.15	3.56	101.8	60.64	1.73	4.45	
	7.5%	9.69	3.82	96.9	56.83	1.52	4.08	
	10%	9.76	4.67	85.4	56.03	1.16	3.89	

Table 3: Tensile properties of the SiO₂-nanocomposites at room temperature and 65°C.

	Percentage of Nanofillers	Young's Modulus (GPa)		Tensile Strength (MPa)		Tensile Strain at break (%)		References
		RT	65°C	RT	65°C	RT	65°C	
PA + GF + SiO ₂	0%	6.92	-	116.2	-	5.2	-	[15]
	0.5%	7.78	-	105.7	-	3.65	-	
	1%	8.40	3	117.8	73.55	4.79	9.12	
	1.5%	7.95	4.46	110.9	67.83	3.43	7.54	
	3%	7.94	4.78	109.5	66.93	3.91	7.45	

Table 4 Quasi-static characteristics of the nanocomposites structures

	Collapse Mode	Initial Peak (kN)	Energy absorbed (kJ)	Specific Energy (kJ/kg)
PA+GF+OMMT 5%	III	42.17	1.752	28.27
PA+GF+ OMMT 7.5%	III	37.57	1.443	22.23
PA+GF+ OMMT 10%	III	35.17	1.562	24.49
PA+GF+ SiO ₂ 0.5%	III	40.04	1.545	24.13
PA+GF+SiO ₂ 1%	III	41.43	1.679	26.34
PA+GF+SiO ₂ 1.5%	III	40.82	1.654	25.72
PA+GF+SiO ₂ 3%	III	40.77	1.619	25.05

Table 5 Dynamic crashing characteristics of the nanocomposites structures

	Crash Length (mm)	Collapse Mode	Initial Peak (kN)	Energy absorbed (kJ)	Specific Energy (kJ/kg)
PA+GF+OMMT 5%	17.87	III	69.86	0.364	12.83
PA+GF+OMMT 7.5%	19.4	II	87.75	0.387	12.60
PA+GF+OMMT 10%	24.23	III	63.40	0.438	12.77
PA+GF+SiO ₂ 0.5%	18.43	II	123.54	0.385	12.98
PA+GF+SiO ₂ 1%	18.01	II	113.46	0.354	13.48
PA+GF+SiO ₂ 1.5%	15.51	II	140.25	0.350	12.54
PA+GF+SiO ₂ 3%	14.76	I	121.40	0.405	14.69

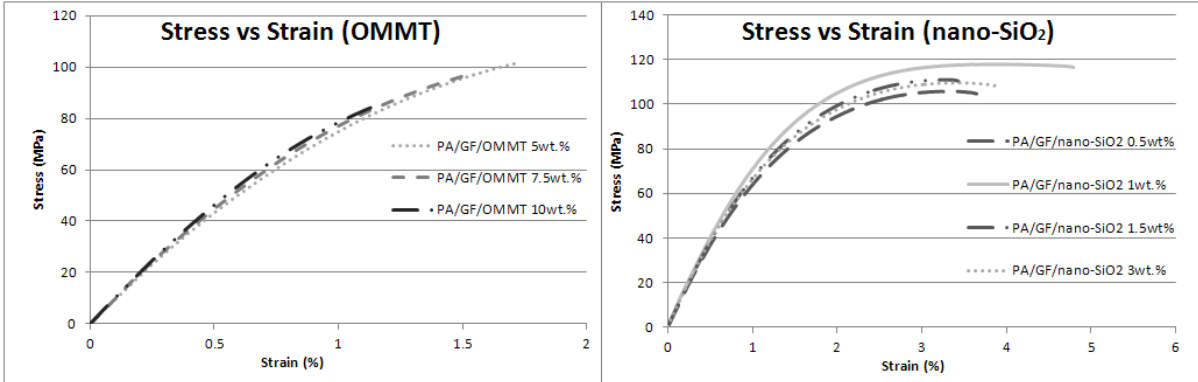


Figure 1: Tensile stress vs tensile strain curves for polyamide-6/glass fibre/OMMT (right) and Polyamide-6/Glass Fibre/SiO₂ at different contents (left).

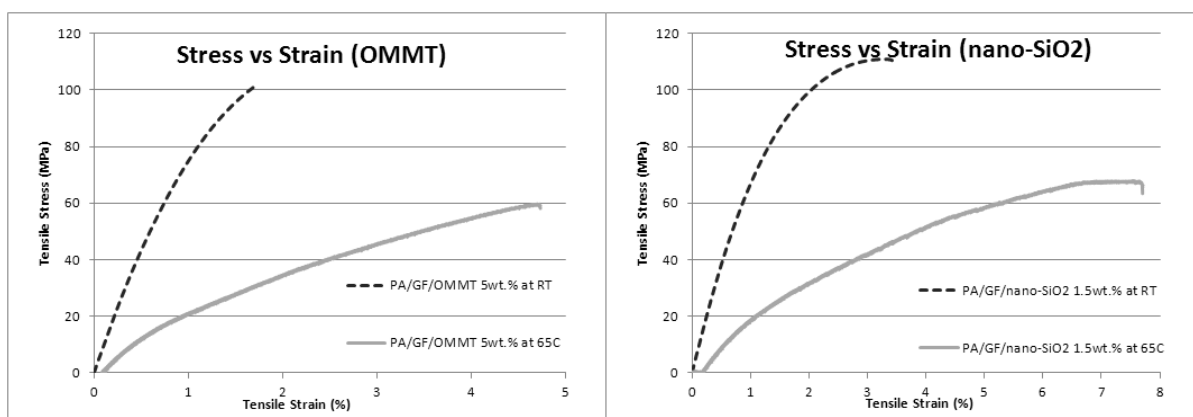


Figure 2: Tensile stress vs tensile strain curves for OMMT-nanocomposites (5 wt.%) and SiO₂-nanocomposites (1.5 wt.%) at room temperature and 65°C.

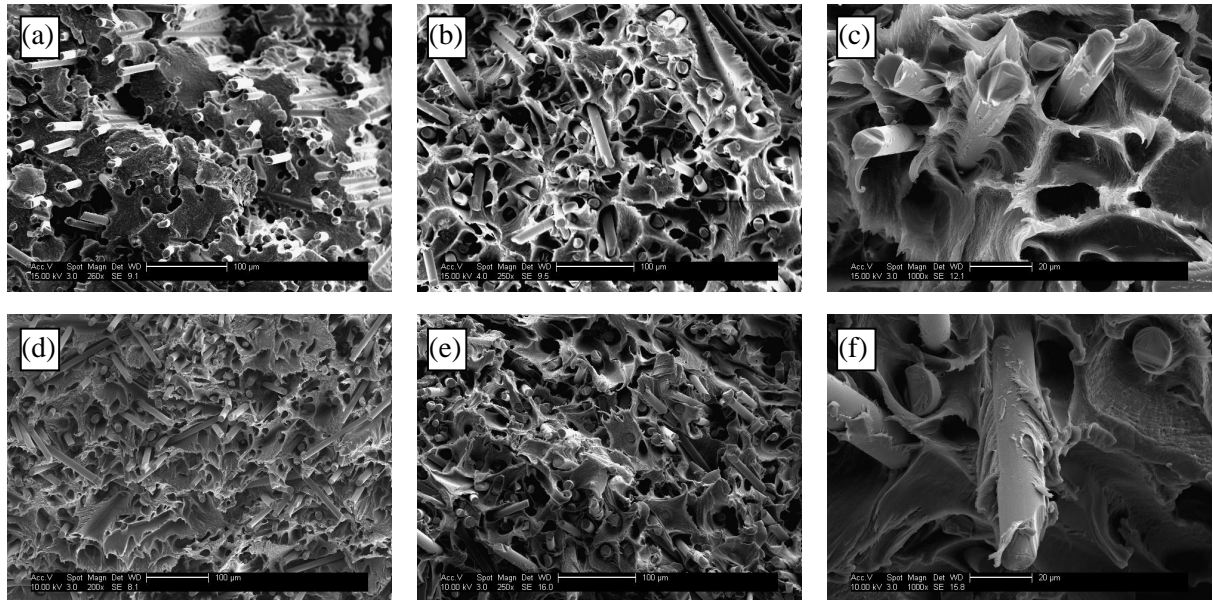


Figure 3: SEM pictures of the tensile fracture surface (a) OMMT-nanocomposite at room temperature, (b) silica-nanocomposite at room temperature, (d) OMMT-nanocomposites at 65°C, (e) silica-nanocomposite at 65°C, and zoom at the glass fibre for silica-nanocomposites (c) at room temperature, and (f) at 65°C.

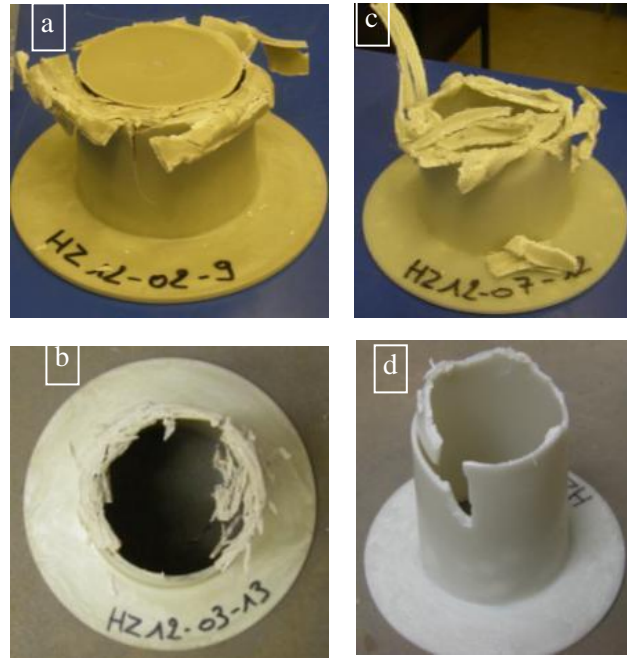


Figure 4 Crash cones reinforced by OMMT, after compression test (a), after crash test (c), reinforced by nano-silica, after compression test (b), after crash test (d)

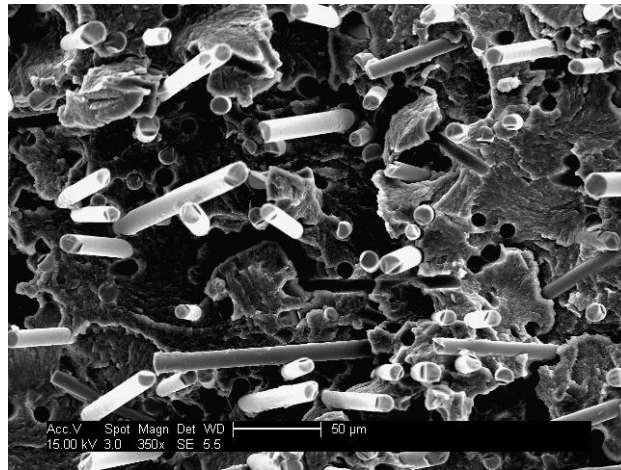


Figure 5: Typical fracture surface of PA6/GF/OMMT samples